Dynamics of the viral community on the cheese surface during maturation and persistence across production years

Thomas Paillet,[a] Quentin Lamy-Besnier,[b] Clarisse Figueroa,[a]* Marie-Agnès Petit,[b] Eric Dugat-Bony[a]#

[a]Université Paris-Saclay, INRAE, AgroParisTech, UMR SayFood, 91120 Palaiseau, France

[b]Université Paris-Saclay, INRAE, AgroParisTech, Micalis Institute, 78352 Jouy-en-Josas, France

Running Head: Viral dynamics and persistence on the cheese surface

#Address correspondence to Eric Dugat-Bony, eric.dugat-bony@inrae.fr.

*Present address: Université de Paris Cité, INSERM, IAME, UMR 1137, 75018 Paris, France

ABSTRACT

The surface of smear-ripened cheeses constitutes a dynamic microbial ecosystem resulting from the successive development of different microbial groups such as lactic acid bacteria, fungi and ripening bacteria. Recent studies indicate that a viral community, mainly composed of bacteriophages, also represents a common and substantial part of the cheese microbiome. However, the composition of this community, its temporal variations and associations between bacteriophages and their hosts remain poorly characterized. Here, we studied a French smear-ripened cheese by both viral metagenomics and 16S metabarcoding approaches to assess both the succession of phages and bacterial communities on the cheese surface during cheese ripening, and their temporal variations in ready-to-eat cheeses over the years of production. We observed a clear transition of the phage community structure during ripening with a decreased relative abundance of viral species (vOTUs) associated with *Lactococcus* phages, which were replaced by vOTUs associated with phages infecting ripening bacteria such as *Brevibacterium*, *Glutamicibacter*, *Pseudoalteromonas* and *Vibrio*. The dynamics of the phage community was strongly associated with bacterial successions observed on the cheese surface. Finally, while some variations in the distribution of phages were observed in ready-to-eat cheeses produced at different dates spanning more than 4 years of production, the most abundant phages were detected throughout. This result revealed the long-term persistence of the dominant phages in the cheese production environment. Together, these findings offer novel perspectives on the ecology of bacteriophages in smear-ripened cheese and emphasize the significance of incorporating bacteriophages in the microbial ecology studies of fermented foods.

IMPORTANCE

The succession of diverse microbial populations is critical for ensuring the production of high-quality cheese. Here, we evidenced a temporal succession of phages, which are viruses infecting bacteria, on the surface of a smear-ripened cheese, with new phage communities showing up at the time where ripening bacteria start covering this surface. Interestingly, the final phage community of this cheese is also consistent over large periods of time, as the same bacteriophages were found in cheese products from the same manufacturer made over 4-years. This research highlights the importance of considering these bacteriophages when studying the microbial life of fermented foods like cheese.

INTRODUCTION

Smear-ripened cheeses develop a typical viscous, red-orange smear on their surface during ripening (1). In France, 14 out of the 46 PDO (Protected Designation of Origin) cheeses belong to this category, *i.e.* Abondance, Beaufort, Chevrotin, Comté, Epoisses, Langres, Livarot, Maroilles, Mont d'Or, Morbier, Munster, Ossau-Iraty, Pont l'Evêque and Reblochon. These cheeses collectively accounted for 61% of the total annual volume of French PDO cheeses marketed, with 128 kilotons in 2021 (https://www.inao.gouv.fr/eng/Publications/Donnees-et-cartes/Informations-economiques). Due to their unique ripening process, involving frequent washes with saline and/or alcoholic solutions, smear-ripened cheeses host a distinct microbiota compared to other cheeses (1). This microbiota is composed of lactic acid bacteria (LAB, mainly starter cultures added at the beginning of the process for milk acidification), yeasts and salt-tolerant bacteria belonging to the Actinomycetota, Bacillota and Pseudomonadota phyla. It is considered to be responsible for the typical flavour and organoleptic properties of this type of cheese (2). Over the past two decades, numerous studies have been conducted to describe the composition of this microbiota using culture-dependent methods (3, 4), molecular fingerprinting (5–8), and more recently amplicon-based metagenomics, also commonly referred to as metabarcoding (9–12).

Time series studies also revealed which microbial succession occur on the surface of smear-ripened cheeses during the maturation process (8, 13, 14). Lactic acid bacteria (LAB), usually originating from starter cultures, grow first in the milk and represent the dominant microorganisms in the curd. Yeasts, *e.g. Debaryomyces hansenii* and *Geotrichum candidum*, which exhibit acid tolerance and metabolize lactate, subsequently colonize the cheese surface, resulting in its deacidification. With the pH increase, the establishment of a diverse bacterial community originating either from raw milk, ripening cultures or the manufacturing environment, is progressively observed. The most common bacterial taxa detected at the end of ripening on smear-ripened cheese belong to coryneform bacteria (*e.g.* species of the *Glutamicibacter*, *Brevibacterium*, *Corynebacterium* or *Brachybacterium* genera), *Staphylococcus* species and halophilic or halotolerant gram-negative bacteria (*e.g.* species of the

Psychrobacter, *Halomonas*, *Pseudoalteromonas*, *Hafnia*, *Vibrio*, *Pseudomonas* or *Proteus* genera) (15).

Microbial successions in cheese during the ripening process result from the interplay between abiotic factors, microbial interactions and complex ecological processes such as dispersion, diversification, environmental selection, and ecological drift (16). While abiotic factors' impact on cheese microbial community assembly has been extensively studied (17, 18), and some important microbial interactions have been revealed as well (19–21), the effects of bacteriophages (or phages), *i.e*. viruses that infect and replicate within bacteria, remain largely understudied. Their role in community assembly has been highlighted in many natural ecosystems (22) and recent work suggests they may affect microbial community dynamics in fermented foods (23, 24), especially through the elimination of key bacterial populations.

In the dairy industry, the impact of LAB phages is well documented because their lytic activity can disturb the milk acidification step, causing delays in the production and even total loss of production (25, 26). Consequently, the most studied dairy phages are *Lactococcus*, *Streptococcus*, *Lactobacillus* and *Leuconostoc* phages, infecting the main starter cultures (27). Viral metagenomics has been recently employed to characterize the bacteriophage communities in dairy samples, including whey (28) and cheeses (29, 30). These investigations have demonstrated that viral communities are not restricted to LAB phages, but encompass a diverse array of phages that could infect non-inoculated and ripening bacteria during cheese production. The recent application of shotgun metagenomics combined with metaHiC on three washed-rind cheeses also enabled to associate hundreds of putative phage contigs with metagenome-assembled genomes (MAGs) of their bacterial hosts, particularly those belonging to Actinomycetota and Pseudomonadota phyla (14).

Beyond metagenomics, only a few studies have documented the isolation of such virulent phages infecting ripening bacteria in cheese, *i.e.* targeting *Propionibacterium freudeunreichii* and *Brevibacterium aurantiacum* (31–33). We recently isolated five additional virulent phages, targeting *Glutamicibacter arilaitensis* (phages Montesquieu and Voltaire), *Brevibacterium aurantiacum* (phage Rousseau), *Psychrobacter aquimaris* (phage d'Alembert) and *Leuconostoc falkenbergense* (phage Diderot), from the surface of a French smear-ripened cheese suggesting that viral infection is likely to

occur on such ecosystems for most of the dominant bacteria (34). However, little is known about their ecology. Specifically, their temporal variations within cheese and their relationships with bacterial successions remain largely unexplored while being essential knowledge to assess the overall impact of phage infections on community assembly.

In this study, we therefore extended our investigations on the same smear-ripened cheese to enhance our understanding of the temporal distribution of bacteriophages and their bacterial hosts on the cheese surface across two distinct timescales (Figure 1). First, cheeses were obtained directly from the production facility at five ripening stages over 28 days (three biological replicates per stage), to analyze phage succession throughout the ripening process (short-term study). Second, ready-to-eat cheeses, *i.e.* after storage and transport to the retail shop, of the same brand and variety were sampled in 2017, 2019, and 2022 (three biological replicates per production year), to assess the temporal variation of the phage community in this ecosystem over the years of production (long-term study). Our results reveal a shift in bacteriophage communities during cheese ripening, correlating with bacterial successions, and highlight the long-term persistence of dominant phages in the studied cheese production system.

RESULTS

Overview of the cheese surface virome dataset.

The viral fraction was extracted from the surface of twenty-four smear-ripened cheese samples (Fig. 1). Fifteen samples were obtained during the ripening process to investigate the ecological succession of phages (short-term study). Nine additional samples were collected post-transport and storage to examine the temporal variation in the phage community across production years (long-term study). Subsequently, the extracted viral fraction was subjected to viral metagenomics techniques.

The cheese viromes had an average sequencing depth of 11,585,587 sequencing reads and were assembled into 5,753 contigs. Viral contigs were selected by considering 2 Kb as the minimum size for viral sequence fragment and by using a combination of viral sequence detection tools (see material and methods section). After clustering based on sequence homology, 331 species-level viral operational taxonomic units (vOTUs) were obtained (Table 1). The vast majority of the vOTUs (*i.e.*

284) were detected in samples from both the short-term and long-term studies. The percentage of reads mapping to these vOTUs reached 91.8% on average, revealing the high quality of virome assemblies. Detailed information about the vOTUs including their size and annotations are available in Table S1. The vOTUs sizes ranged from 2,002 to 144,530 bp, 79 contigs (24%) being >10 Kb (Fig. 2A). This included 25 vOTUs (7.6%) flagged as complete genomes and 12 (3.6%) as high-quality genomes according to CheckV (35). Twenty-seven vOTUs (8.2%) were identified as temperate phages by Vibrant (36) if they were excised from a larger contig or if they encode an integrase. A bacterial host was successfully predicted at the genus level for most vOTUs (272/331, *i.e.* 82.2%), spanning three bacterial phyla, namely Actinomycetota, Bacillota and Pseudomonadota (Fig. 2B). *Lactococcus* was the predicted genus containing the highest phage diversity (182 vOTUs), followed by *Leuconostoc* (23 vOTUs). *Pseudoalteromonas* (18 vOTUs), *Psychrobacter* (17 vOTUs) and *Brevibacterium* (6 vOTUs). Only 40.4% of vOTUs (134/331) shared sequence homology (>30% identity × coverage based on BLAT score) with a known dairy phage (Table S2). However, those vOTUs represented 97% of the relative abundance observed in the dataset (Table 2) showing that most of the dominant phages present in this ecosystem have isolated and characterized relatives. Among them were present *Lactococcus* phages from the 949 (*Audreyjarvisvirus* genus), 936 (*Skunavirus* genus) and P335 groups, as well as the five virulent phages isolated from the same type of cheese (same variety, same brand) in our previous work (34), namely *Glutamicibacter* phages Montesquieu and Voltaire, *Brevibacterium* phage Rousseau, *Psychrobacter* phage D'Alembert and *Leuconostoc* phage Diderot (*Limdunavirus* genus).

Successional dynamics of the cheese virome throughout the ripening process.

After phage identification, our next objective was to follow the phage communities throughout the ripening process, with a particular focus on the washing steps (short-term study). In the manufacturing process of the studied cheese, the first three washing operations (named W1, W2 and W3) utilize a NaCl solution, while the last two operations (W4 and W5) utilize a NaCl solution containing increasing concentrations of alcoholic liquor (Fig. 1). The dataset consisted in 15 samples (triplicate samples for each washing operation) and 318 vOTUs (Table 1).

The viral diversity was estimated by the Shannon index, which varied from 2.631 to 3.442 across samples (median = 2.969). A slight but non-significant ($p > 0.05$, Kruskal-Wallis test; Fig. 3A) decrease in the Shannon index was noted from W3 onwards, suggesting there was no major alteration of the viral diversity during ripening. An overall sparsity of 29% (percentage of 0 values in the matrix) was observed on the abundance table reflecting that all the studied cheese viromes shared most of the detected vOTUs. However, structural variation in the virome composition was assessed by computing Bray-Curtis dissimilarity (Fig. 3B) and the PERMANOVA test indicated a significant effect of the washing operation ($p = 0.001$, $r^2 = 0.658$).

To explore further this change, we selected vOTUs with a normalized relative abundance above 0.005 % on average (168 contigs) and represented their distribution across samples in a heatmap (Fig. 3C). A clear change in the structure of the vOTUs distribution appeared over time. Based on the total within sum of square (Fig. S1), we delineated five vOTUs clusters (labelled I to V in Fig. 3C). Clusters I and II were characterized by vOTUs whose abundance did not vary with the ripening and that corresponded mainly to virulent *Lactococcus* phages belonging to the 936 group (*Skunavirus* genus). Cluster V contained vOTUs whose abundance decreased with ripening and that corresponded to other *Lactococcus* phages, close to the P335 group containing both temperate and virulent members. Finally, clusters III and IV were essentially composed of a few vOTUs that increased in relative abundance with ripening. These mainly corresponded to phages targeting ripening bacteria such as *Brevibacterium*, *Glutamicibacter*, *Pseudoalteromonas* and *Vibrio*, and non-starter lactic acid bacteria (NSLAB) such as *Leuconostoc*. These few vOTUs corresponded to uncharacterized phages, except *Glutamicibacter* phage Montesquieu, *Brevibacterium* phage Rousseau and *Leuconostoc* phage Diderot which we previously isolated from the same type of cheese (34).

Both the principal coordinate analysis of the Bray-Curtis dissimilarity (Fig. 3B) and the heatmap visualization (Fig. 3C) revealed a comparable virome composition between samples collected from W1 and W2, as well as between those from W4 and W5. This observation suggests the succession of two predominant viral communities on the cheese surface during the ripening process, corresponding to these respective stages. Samples from W3 displayed a unique and typically intermediate composition. In these samples, clusters III and IV were found in higher relative

abundance compared to W1-W2 but not as abundant as in W4-W5. Cluster V was also detected in lower abundance than in W1-W2 but at a level similar to W4-W5.

We finally applied the DESeq2 method (37, 38) to statistically identify which vOTUs differentiate the two predominant viral communities represented by W1-2 and W4-5 samples (Fig. S2). In total, 22 vOTUs were differentially abundant between the two communities (adjusted $p < 0.05$, log2 fold change >3 or <-3). Interestingly, two groups of vOTUs emerged with readable outcomes: vOTUs of the phages infecting starter cultures, such as *Lactococcus* and *Streptococcus* phages, had a negative log2 fold change, meaning their relative abundances significantly decreased during the ripening process. Conversely, vOTUs of virulent phages targeting NSLAB and ripening bacteria (e.g. *Brevibacterium, Glutamicibacter, Pseudoalteromonas* and *Vibrio*) as well as unknown phages were significantly more abundant in W4-5 samples compared to W1-2 samples (positive log2 fold change), reflecting their higher population level in the later ripening stages. Among them were two vOTUs with high similarity to *Glutamicibacter* phage Montesquieu (2017-3_NODE2; 47,703 bp; 100% identity × coverage by BLAT), and *Brevibacterium* phage Rousseau (2022-5_NODE4; 41,077 bp; 54% identity × coverage by BLAT but 98% identity at the nucleotidic level over a portion of >9 kb). In this group, we also detected a vOTU partially related to *Brevibacterium* phage AGM1 (SA2-0_NODE10; 37148 bp; 3.5% identity × coverage by BLAT but 88% identity at the nucleotidic level over a portion of 1324 nt), which was isolated from a Canadian washed-rind cheese (32).

Relationships between cheese virome and bacteriome throughout the ripening process.

Having observed a succession of viral communities on the cheese surface during the ripening process, we sought to investigate how it was associated with bacterial community changes. We therefore profiled bacterial communities on the same samples using 16S metabarcoding. A total of 773,059 reads were obtained and clustered into 195 operational taxonomic units (OTUs) assigned to 14 different bacterial genera (Fig. 4A). As observed for viruses, the composition of the bacteriome of the cheese surface varied through the ripening process and a clear transition in the bacterial community structure was detected from W3 onwards. *Lactococcus* was the dominant genus in samples

from W1 and W2, and was progressively overgrown by typical surface aerobic bacteria such as members of *Psychrobacter*, *Vibrio*, *Glutamicibacter* and *Pseudoalteromonas* genera.

As metabarcoding data provide only relative proportions, bacterial counts were performed to introduce a quantitative aspect to the bacterial dynamics (Fig. 4 B and C). We observed an approximately 2-log increase in aerobic bacteria between W1 and W5, rising from ~ 10^8 to ~ 10^{10} CFU/g. In contrast, lactic acid bacteria remained stable over time (~ 10^8 CFU/g) throughout the entire experiment. We concluded that the observed change in the relative abundance of *Lactococcus* sequences through metabarcoding was primarily attributed to the growth of aerobic bacteria.

A Mantel test demonstrated the statistical relationships between the virome and bacteriome datasets (p = 0.001; r = 0.3151; 999 permutations). This indicates that changes observed on the phage community structure are associated with bacterial successions on the cheese surface. We further calculated Spearman correlations between the relative abundances of the main phage groups identified in the metavirome and of bacterial genera in the bacteriome to identify co-abundance or mutual-exclusion patterns (Fig. 4D). We observed several positive correlations between phages and their bacterial host genus. For example, *Psychrobacter* phage d'Alembert and *Glutamicibacter* phage Montesquieu exhibited positive correlations with several ripening bacteria including *Psychrobacter* and *Glutamicibacter* genera. *Brevibacterium* phage Rousseau correlated also with the same bacterial genera but not with *Brevibacterium*, likely due to its low detection level in the studied cheese. LAB phages belonging to KSY1, P335 and 987 groups, which are infecting *Lactococcus lactis* and/or *Streptococcus thermophilus*, were positively correlated with *Lactococcus* genus.

Temporal variation of the cheese virome across production years.

As phage succession was evidenced in the short-term, specifically during the ripening process, we next wanted to test whether the composition of the virome remained comparable over multiple years of cheese production. To address this, we analyzed the long-term dataset comprising 297 vOTUs detected on nine cheese samples of the same type and brand as the ones used for the short-term study (Table 1). These samples were collected after ripening, transport and storage across three different production years (Fig. 1). We first focused on determining the proportion of vOTUs shared across

production years. Utilizing the full dataset without relative abundance filtering, we observed that 56.6% of the vOTUs (168) were consistently detected in all production years, with 75.4% (224) observed in at least two different production years (Fig. 5A). Notably, samples from the year 2022 had a higher number of unique vOTUs (48, 32.1% of the total) compared to samples from the years 2017 and 2019 (3 and 11, respectively). We also conducted the same analysis focusing on the most abundant vOTUs, defined by an average normalized relative abundance > 0.005% (99 vOTUs in total) (Table 1, Fig. 5B). A large majority of the vOTUs, *i.e.* 89.9%, were shared across all three production years and this value rose to 97% when considering only two different years. This underscores the stability of the cheese surface virome in terms of composition (presence/absence) and emphasizes the long-term persistence of dominant phages in the studied ecosystem.

The effect of the production year (2017, 2019 and 2022) on the structure of the cheese virome was further investigated by computing Bray-Curtis dissimilarity on the vOTU abundance table without relative abundance filtering (Fig. 5C). The principal coordinate analysis revealed a distinct grouping of samples consistent with the production years. The first axis discriminated samples from year 2019 and samples from years 2017 and 2022. The second axis discriminated samples from years 2017 and 2022. The PERMANOVA test confirmed a significant effect of the production year (p = 0.002, R^2 = 0.814) on the distance metrics indicating structural variations of the phage community across production years. Given the consistent presence of the most abundant vOTUs across all production years (Fig. 5B), such variations could be attributed to the fluctuations in the presence/absence of phages with lower abundance, as well as to the distribution of dominant phages in terms of relative abundances.

Heatmap visualization was then used to identify phages explaining such structural variations (Fig. 5E) in combination with differential abundance analysis (Fig. S3). Whereas the general profiles of all the viromes were very similar, a few vOTUs were more specifically detected in one or two production years. For example, the second most abundant vOTU in 2017 and 2019 (SS2-4_NODE1) which is highly similar to *Lactococcus* phage 949 (*Audreyjarvisvirus* genus) was statistically less abundant in 2022 (adjusted p <0.05, log2 fold change <-3) contrary to a group of other distinct vOTUs also predicted to infect *Lactococcus* but either not identified, or assigned to the 936 (*Skunavirus* genus) and P335 groups. Regarding *Psychrobacter* phages, the vOTU closely related to phage

d'Alembert (2017-0_NODE1) was more abundant in 2017 than in the two other years (adjusted p <0.05, log2 fold change >3). However, two vOTUs without sequence homology with known dairy phages, but predicted to infect also *Psychrobacter* (2022-0_NODE3 and 2022-5_NODE3), were detected later in 2022 in higher abundance (adjusted p <0.05, log2 fold change >3). Notably, *Glutamicibacter* phage Voltaire was present in low abundance in 2017 and 2019 (0.036% and 0.004% relative abundance on average, respectively), but was not detected in 2022.

We also performed 16S metabarcoding analysis to determine whether compositional changes were observed in the bacterial community as well. The surface of the studied smear-ripened cheese was characterized by ten dominant bacterial genera. Similar to what we observed for phages, these genera were consistently detected in all samples (Fig. 5D). However, variations in their relative abundance were detected across the three production years.

Together, our results indicate the presence of a core microbiome consisting of dominant microorganisms and their associated viruses that define the surface of the cheese under study. The composition of this core microbiome seems to persist in the long-term timescale, although changes in the microbial balance can be observed between production batches.

DISCUSSION

Recent studies of cheese samples using viral metagenomics (29, 30) or exploration of cheese microbial metagenomes (14, 39) have revealed that the cheese environment harbours a diverse bacteriophage community whose targets go beyond lactic acid starter cultures. The previous isolation of a few representatives of these non-starter phages (32–34) suggests that phage infection occurs in this ecosystem during the ripening process. Recently, the deliberate addition of one of those phages, *Brevibacterium* phage AGM9, was proven to slow down the development of the orange rind color in a model system mimicking a smear-ripened cheese (40). In the present study, we described the temporal variation of the viral community of a French smear-ripened cheese at two timescales: short-term (28 days corresponding to the duration of the ripening process) and long-term (spanning four years of production). The virome was predominantly composed of vOTUs associated with a variety of *Lactococcus* phages as well as the *Glutamicibacter* phage Montesquieu, a virulent phage we had

previously isolated from the same cheese variety (34). This phage targets the ripening bacterium *Glutamicibacter arilaitensis*.

Several other known dairy phages, such as *Brevibacterium* phage Rousseau, *Leuconostoc* phage Diderot, *Psychrobacter* phage d'Alembert, *Glutamicibacter* phage Voltaire, and a novel vOTU displaying minimal sequence homology to *Brevibacterium* phage AGM1 were also detected, but at lower abundance. Notably, while known dairy phages represented 97% of the relative abundance in our dataset, 197 vOTUs (59.6% of the total) remained unidentified and 49 (17.8%) had no predicted host. The diversity of these low-abundant phages is therefore not yet completely sampled and, in particular, our results underscore the necessity to isolate a more comprehensive collection of phages from cheese and other fermented foods in general. For example, a few vOTUs partially aligned with genomic sequences from phages infecting halotolerant bacteria but isolated from natural environments (e.g., *Pseudoalteromonas*, *Halomonas*, *Vibrio*, and *Proteus* species). Even though these bacteria are not intentionally inoculated into smear-ripened cheese, they are frequently detected in such products and tend to dominate by the end of the ripening process (15). Their phages should therefore be looked for in future isolation initiatives.

The dynamics of bacterial and fungal communities have been extensively studied in a wide diversity of cheese products during ripening (13, 41–45), enabling us to accurately describe the successions of cellular organisms occurring in cheese production processes (16). In this study, we present the first analysis of viral dynamics throughout cheese ripening. Similar to the observed transitions in bacteria and fungi, there was a distinct shift in viral composition throughout the ripening process. Some vOTUs associated with LAB starter phages, primarily targeting *Lactococcus lactis*, were progressively replaced by vOTUs specific to phages that infect ripening bacteria. We observed a strong correlation between the dynamics of phage and bacterial communities during the ripening process. Specifically, the relative abundance of several phages, such as *Glutamicibacter* phage Montesquieu, *Psychrobacter* phage d'Alembert and *Lactococcus* phages belonging to the 936 (*Skunavirus* genus), KSY1 and P335 groups was positively correlated to the relative abundance of their predicted bacterial hosts. This observed positive correlation contrasts with the anticipated negative correlation that might have been expected if virulent phages were responsible for eliminating

key members of the bacterial community during cheese ripening. This result therefore raises questions about the overall impact of phages on bacterial successions in cheese during ripening. However, it is important to note that phage susceptibility is generally strain-dependent, as demonstrated in previous studies on LAB strains (summarized in (46)) and in undefined starter cultures where multiple strains of the same species stably co-exist with distinct phages (47–49). The narrow host range observed for phages infecting ripening bacteria recently isolated from cheese rind also corroborates this result (32, 34). In the present work, the composition of the bacterial community was assessed at the genus level, thus preventing capturing such strain-level diversity. Future investigations at strain level would therefore be highly relevant to better understanding the ecological role of phages in cheese rind microbial communities.

Surprisingly, despite the changes in bacterial and viral communities' composition during the production process, the relative abundance of some vOTUs remained very stable during ripening. They mainly corresponded to virulent *Lactococcus* phages, belonging to the *Skunavirus* genus (formerly 936 group). Among *Lactococcus* phages, this genus is by far the most frequently detected in the dairy industry (50). Given that *Lactococcus lactis* predominantly proliferates during milk acidification and maintains consistent concentration levels throughout ripening in this type of cheese (13), we theorize that the maintenance of *Skunavirus* is indicative of the stability of phage particles produced at the onset of cheese maturation. The remarkable stability of *Skunavirus* particles in comparison to other *Lactococcus* phage groups, especially the P335 group, has been reported earlier (51, 52). In contrast, we suggest that the relative decline observed in our experiment for other *Lactococcus* phages, specifically those affiliated with the P335 group, denotes their temporal instability. Nevertheless, a more comprehensive examination of this phenomenon warrants dedicated investigations.

Microbial communities of washed-rind cheese are generally dominated by environmental microorganisms detected in processing environments, the so-called "house" microbiota (53), which is specific to each production facility and provides a microbial signature distinguishing cheeses belonging to the same variety but manufactured by distinct producers (10). Recently, the analysis of

several of Quebec's terroir cheeses revealed that the dominant microorganisms remain stable from year to year, which could be linked to typical manufacturing practices and consistency in the use of starter and ripening cultures by cheesemakers (54). Here, we describe a similar observation for bacteriophages. We indeed identified a core virome composed of the most abundant vOTUs, consistently detected in three different years of production. Previous work on an undefined starter culture used for the production of a Swiss-type cheese propagated for decades in the same dairy environment, revealed that phages and bacteria stably coexist over time in this system and suggests that this may contribute to the stable maintenance of the cheese starter culture over years (47). Phages and ripening bacteria present on the surface of natural smear-ripened cheese are contaminating the cheese production environment, and are therefore likely to repeatedly contaminate cheese from one production cycle to another (34, 53). Nevertheless, further research is needed to elucidate the contributions of phages to both the long-term maintenance of the strain-level diversity of ripening bacteria and the occurrence of punctual microbial disequilibrium leading to organoleptic defects. These findings may be specific to the type of cheese under study, the strain-level diversity of the main bacteria, and the operational conditions used for cheese production.

In conclusion, the observed dynamics of the cheese virome throughout the ripening process, coupled with the persistence of the most dominant phages across production years, support the important role of bacteriophages in the cheese microbial ecosystem. The acquisition of new knowledge about phage ecology is now essential for a comprehensive understanding of microbial successions during milk fermentation. Moreover, this knowledge may offer cheesemakers novel avenues to refine and control their production processes.

MATERIAL AND METHODS

Cheese samples.

(i) Short-term study design: French smear-ripened cheeses, all from the same production batch, were collected directly from a cheese plant at five different stages during the ripening process (Figure 1). Three different cheeses were sampled per stage, and considered as biological replicates. The stages,

labeled W1 to W5, correspond to distinct washing steps. The initial three washes utilized a NaCl solution, while the final two employed a NaCl solution supplemented with increasing concentrations of alcoholic liquor (standard alcohol concentration of 40%). At each stage, three distinct cheeses were sampled and designated as biological replicates A, B, and C. Cheeses were immediately stored at 4°C after sampling and processed within 48h.

(ii) Long-term study design: ready-to-consume cheeses of the same type and brand as the previously described cheeses were purchased in a local supermarket in December 2017, November 2019 and February 2022, spanning >4 years of production (Figure 1). Three different cheeses, with the same production date, were sampled each year and used as biological replicates. Cheeses were immediately stored at 4°C after sampling and processed within 48h.

For both short-term and long-term studies, cheese samples were analyzed immediately after reception at the lab. Using sterile knives, the rind, approximately 2-3 mm thick, was carefully separated from the core. It was then blended and processed for microbial counts, viral DNA extraction for metavirome analysis, and microbial DNA extraction for extensive amplicon sequencing targeting the 16S rRNA gene, which will be subsequently referred to as 16S metabarcoding.

Microbiological analysis.

Bacteria were enumerated by plating serial dilutions (10^{-1} to 10^{-7}) of one gram of cheese rind mixed in 9 mL of physiological water (9 g/L NaCl) on two different culture media as described in our previous study (29). Brain Heart Infusion Agar (BHI, Biokar Diagnostics) supplemented with 50 mg/L amphotericin (Sigma Aldrich, Saint-Louis, MO, USA) was used to count total aerobic bacteria after 48 h of incubation at 28°C. Man, Rogosa and Sharpe Agar (MRS, Biokar Diagnostics, Allonne, France) supplemented with 50 mg/L amphotericin was used to count lactic acid bacteria after 48 h of incubation at 30°C under anaerobic conditions.

Viral DNA extraction and metavirome analysis.

Extraction of the viral fraction from the cheese rind was performed according to protocol P4 detailed in (29) including a filtration step and a chloroform treatment. DNA was extracted from the viral particles according to the protocol described in the same study and sent to Eurofins Genomics for high throughput sequencing using the Illumina NovaSeq platform (2 × 150 bp paired-end reads,

approximately 10 million reads per sample). The experimental procedures used for nucleic acids extraction and sequencing library preparation limited this study to the description of double-stranded DNA viruses, excluding single-stranded DNA and RNA viruses.

All the details about the tools, versions and parameters used in the following pipeline are available in scripts deposited in the GitLab repository (https://forgemia.inra.fr/eric.dugat-bony/cheese_virome). Briefly, raw reads were quality-filtered using Trimmomatic v0.39 (55). Then a single assembly was computed for the collection of triplicate reads from each sample with Spades v3.15.3 (56), using either the complete dataset of trimmed reads available or after subsampling the dataset to 1.5 million, 150,000 or 15,000 trimmed reads per sample. We noted that some abundant contigs were assembled into longer, nearly complete contigs, after subsampling. Among the 5,753 contigs, those >2kb were selected and clustered following an approach adapted from (57). Succinctly, a pairwise alignment was first performed for all contigs using BLAT (58). Then, contigs with a self-alignment > 110% of contig length, corresponding to chimeras, were removed. The remaining contigs were clustered at the species level (90% identity × coverage) and the longest contig within each cluster was selected as the representative sequence. The final contig dataset consisted of 3,122 dereplicated contigs.

Among them, 332 were identified of viral origin (vOTUs) by using a combination of three detection tools: VIBRANT v1.2.1 (36), VirSorter2 v2.2.4 (59) and CheckV v0.8.1 (35). To be declared as viral, a contig had to meet at least one of the following criteria: declared “complete”, “high” or “medium” quality by either VIBRANT or CheckV, declared “full” by VirSorter2. The bacterial host of the vOTUs was predicted using iPHoP (60). Finally, all sequences were compared by BLAT to an in-house database consisting of genome sequences from 32 common dairy phages (listed in Table S1) to identify potentially related phages with known taxonomy, verified host and lifestyle (30% identity × coverage minimal cutoff). When appropriate, the host genus predicted by iPHoP was replaced by the genus of the bacterial host of the closest relative phage identified by the BLAT search. One vOTU, corresponding to the genome of the phage PhiX174 which is routinely used as control in Illumina sequencing runs to monitor sequencing quality, was discarded resulting in a final dataset of 331 vOTUs.

To evaluate the relative abundance of each vOTU in each metavirome sample, trimmed reads were mapped against the vOTUs using bwa-mem2 v2.2.1 (61) and counted with Msamtools v1.0.0 profile with the options --multi=equal --unit=ab –nolen (https://github.com/arumugamlab/msamtools). The output files from all samples were joined into an abundance table and processed using the R package phyloseq v1.38.0 (62). For each experimental dataset (short-term and long-term studies), read counts were rarefied to the minimum depth observed in one individual sample. To facilitate comparison of abundance levels among vOTUs, read counts were divided by contig length resulting in an abundance table containing the mean coverage per vOTU in each sample. Subsequently, normalization of the table was conducted using the total sum scaling method (TSS) (63), which simply transforms the abundance table into a relative abundance table through scaling by each sample's library size, thus enabling comparisons between samples. Assuming that one vOTU corresponds to one species (which is wrong each time several contigs belonging to the same phage genome are present), Bray-Curtis dissimilatory index, as computed by the distance function from the R package phyloseq, was used to compare viral communities between samples and the effect of different variables on their structure was assessed using permutational analysis of variance (PERMANOVA) as computed by the adonis2 function from the R package vegan v2.6-2.

Differential analysis was performed using the DESeq function implemented in the R package DESeq2 v1.38.0 (37) for which an official extension exists within the R package phyloseq (https://joey711.github.io/phyloseq-extensions/DESeq2.html). This method was shown to perform well in the detection of differentially abundant taxa in microbiome data (38). Because the DESeq function already includes a normalization step (by the median of ratios method), this analysis started from raw counts. The Wald test was used for comparing the abundance of all vOTUs between two sample groups and vOTUs were considered differentially abundant if the p value was < 0.01 after correction for multiple testing using the Benjamini and Hochberg method, log2 fold change was > 3 or -3 and average raw counts was > 1500.

Microbial DNA extraction and 16S metabarcoding profiles.

Total DNA extraction from the cheese surface was performed as previously described (10). PCR amplification of the V3-V4 regions of the 16S rRNA gene was performed with the primers V3F (5'-

ACGGRAGGCWGCAG-3') and V4R (5'-TACCAGGGTATCTAATCCT-3') carrying the Illumina 5'-CTTTCCCTACACGACGCTCTTCCGATCT-3' and the 5'-GGAGTTCAGACGTGTGCTCTTCCGATCT-3' tails, respectively. The reaction was performed using 10 ng of extracted DNA, 0.5 µM primer, 0.2 mM dNTP, and 2.5 U of the MTP Taq DNA polymerase (Sigma-Aldrich, USA). The amplification was carried out using the following program: 94°C for 60 s, 30 cycles at 94°C for 60 s, 65°C for 60 s, 72°C for 60 s, and a final elongation step at 72°C for 10 min. The resulting PCR products were sent to the @BRIDGe platform (INRAE, Jouy-en-Josas, France) for library preparation and sequencing. Briefly, amplicons were purified using magnetic beads CleanPCR (Clean NA, GC biotech B.V., The Nederlands), the concentration was measured using a Nanodrop spectrophotometer (Thermo Scientific, USA) and the amplicon quality was assessed on a Fragment Analyzer (AATI, USA) with the reagent kit ADNdb 910 (35-1,500 bp). Sample multiplexing was performed by adding tailor-made 6 bp unique indexes during the second PCR step which was performed on 50–200 ng of purified amplicons using the following program: 94°C for 10 min, 12 cycles at 94°C for 60 s, 65°C for 60 s, 72°C for 60 s, and a final elongation step at 72°C for 10 min. After purification and quantification (as described above), all libraries were pooled with equal amounts to generate an equivalent number of raw reads for each library. The DNA concentration of the pool was quantified on a Qubit Fluorometer (Thermofisher Scientific, USA) and adjusted to a final concentration between 5 and 20 nM for sequencing. The pool was denatured (NaOH 0.1N) and diluted to 7 pM. The PhiX Control v3 (Illumina, USA) was added to the pool at 15% of the final concentration, as described in the Illumina procedure, and the mixture was loaded onto the Illumina MiSeq cartridge according to the manufacturer's instructions using the MiSeq Reagent Kit v3 (2 × 250 bp paired-end reads).

Paired-end reads were analyzed using FROGS v3.2 (64), according to the standard operating procedure. Briefly, operational taxonomic units (OTUs) were built using Swarm with an aggregation distance of 1 and the --fastidious option (65), and each OTU that accounted for <0.005% of the total dataset of sequences was discarded, as previously recommended (66). Lastly, OTU affiliation was checked using the EzBiocloud database v52018 (67). The abundance table was processed using the R package phyloseq v1.38.0 (62).

Data availability.

Raw sequencing data for cheese virome and bacterial microbiome were deposited at the sequence read archive (SRA) of the NCBI (https://www.ncbi.nlm.nih.gov/sra/) as part of bioprojects PRJNA984302 (short-term study) and PRJNA984735 (long-term study).

ACKNOWLEDGMENTS

T.P. is the recipient of a doctoral fellowship from the French Ministry of Higher Education, Research and Innovation (MESRI) and the MICA department of the French National Research Institute for Agriculture, Food and Environment (INRAE). For the metabarcoding analysis, this work has benefited from the facilities and expertise of @BRIDGe (Université Paris-Saclay, INRAE, AgroParisTech, GABI, 78350 Jouy-en-Josas, France). We are also grateful to the INRAE MIGALE bioinformatics facility (MIGALE, INRAE, 2020. Migale Bioinformatics Facility, doi: 10.15454/1.5572390655343293E12) for providing computing and storage resources.

TABLES

Table 1: summary statistics about the metavirome dataset.

	Complete dataset (24 samples)	**Short-term study (15 samples)**	**Long-term study (9 samples)**
Total number of vOTUs > 2 Kb	331	318	297
Number of vOTUs with relative abundance > 0.005%	157	168	99
Percentage of reads mapping against vOTUs (± SD)	91.8 ± 12.1	94.3 ± 7.0	87.6 ± 17.4

Table 2: Most abundant dairy phages detected on the cheese metavirome. Phages that have been previously isolated from the same cheese variety are highlighted in bold. When classification is

available at the International Committee on Taxonomy of Viruses (ICTV), the viral genus is denoted in parenthesis.

Closest relatives	**Relative abundance***
Lactococcus 949 group *(Audreyjarvisvirus)*	0.56
***Glutamicibacter* Montesquieu**	**0.23**
Lactococcus 936 group *(Skunavirus)*	0.18
Lactococcus P335 group	1.54E-03
***Brevibacterium* Rousseau**	**1.08E-03**
***Psychrobacter* D'Alembert**	**1.74E-04**
Leuconostoc* Diderot *(Limdunavirus)	**1.14E-04**
***Glutamicibacter* Voltaire**	**1.70E-05**
Streptococcus 987 group	7.87E-06
Lactococcus KSY1 group *(Chopinvirus)*	5.94E-07
Non-dairy phages**	0.03

*The relative abundance value used here is not normalized by genome size, it corresponds to the relative proportion of reads mapping to all vOTUs belonging to a given phage group present in our in-house dairy phage database (Table S1).

**vOTUs without any match to our in-house dairy phage database (30% identity × coverage minimal cutoff).

FIGURE LEGENDS

Figure 1: Schematic representation of the experimental plan followed for the study of temporal variation in the cheese virome composition. For the short-term study, cheese samples were collected in triplicate after each washing operation during the ripening process (blue arrows indicate washes performed with a NaCl solution, while red arrows indicate washes performed with a NaCl solution containing alcoholic liquor). For the long-term study, cheese samples were collected in triplicate after

storage and transport at three different production years. All samples were analyzed through viral metagenomics, 16S metabarcoding and microbial plate counts.

Figure 2: Characteristics of the cheese virome dataset. A) Size distribution of the vOTUs. B) Distribution of the vOTUs per bacterial host genus.

Figure 3: Viral succession on the cheese surface throughout the ripening process. A) Comparison of the viral diversity, estimated by the Shannon index, at the different ripening steps. B) Principal coordinate analysis of the Bray-Curtis dissimilarity. Samples are colored according to the washing operation. C) Heatmap representing the normalized relative abundance of the most abundant vOTUs in the different samples. The colors on the heatmap represent the log-transformed relative abundance and range from blue (low relative abundance) to red (high relative abundance). Host genus, phage group and lifestyle of the different vOTUs are indicated when available. Hierarchical clustering using the complete linkage method was used to define the order of rows (vOTUs). The five vOTUs clusters detected in the dataset are boxed in red and labelled I to V.

Figure 4: Relationship between phage succession and the composition of cheese bacterial community during the ripening process. A) Composition of the bacterial community assessed by a metabarcoding approach targeting the V3-V4 regions of the 16S rRNA gene. Three different cheeses from the same batch were analyzed at each sampling point. Data were aggregated at the genus level. B) Aerobic bacteria counts expressed in log(CFU/g). C) Lactic acid bacteria counts expressed in log(CFU/g). D) Heatmap of Spearman correlations (*r* values, ranging from -1 to +1) describing the relationship between the main phage groups detected in the virome dataset and bacterial genus-level relative abundances. Hierarchical clustering using the complete linkage method was used to define the order of rows (bacterial genera) and columns (phage groups).

Figure 5: Temporal variation of the cheese surface virome across production years. A) Venn diagram constructed from the dataset without filtering, comprising 297 vOTUs. B) Venn diagram

constructed from the filtered dataset comprising 99 vOTUs with an averaged normalized relative abundance value > 0.005%. C) Principal coordinate analysis of the Bray-Curtis dissimilarity. Samples are colored according to the production year (2017, 2019 and 2022). D) Composition of the bacterial community assessed by a metabarcoding approach targeting the V3-V4 regions of the 16S rRNA gene. Three different cheeses from the same production year were analyzed. Data were aggregated at the genus level. E) Heatmap representing the normalized relative abundance of the most abundant vOTUs in each sample. The colors on the heatmap represent the log-transformed relative abundance and range from blue (low relative abundance) to red (high relative abundance). Host genus, phage group and lifestyle of the different vOTUs are indicated when available. Hierarchical clustering using the complete linkage method was used to define the order of rows (vOTUs).

SUPPLEMENTARY MATERIAL

Table S1. Detailed annotation of the viral operational taxonomic units.

Table S2. Common dairy phages and associated information.

Figure S1: Estimation of the optimal number of vOTUs clusters in the short-term dataset. The total within-cluster-sum-of-square was calculated for each number of clusters and the elbow point was used to determine the optimal number of clusters.

Figure S2: Differential abundance analysis of the virome data between the two stable stages represented by W1-2 and W4-5 samples (short-term study). Log2 fold change values obtained for differential abundant vOTUs (dots) are represented and the dot color indicates the predicted host genus.

Figure S3: Differential abundance analysis of the virome data between the three years of production (long-term study). A) Comparison between years 2017 and 2019. B) Comparison between years 2017 and 2022. C) Comparison between years 2019 and 2022. Log2 fold change values

obtained for differential abundant vOTUs (dots) are represented and the dot color indicates the predicted host genus.

REFERENCES

1. Mounier J, Coton M, Irlinger F, Landaud S, Bonnarme P. 2017. Chapter 38 - Smear-Ripened Cheeses, p. 955–996. *In* McSweeney, PLH, Fox, PF, Cotter, PD, Everett, DW (eds.), Cheese (Fourth Edition). Academic Press, San Diego.

2. Corsetti A, Rossi J, Gobbetti M. 2001. Interactions between yeasts and bacteria in the smear surface-ripened cheeses. International Journal of Food Microbiology 69:1–10.

3. Larpin-Laborde S, Imran M, Bonaïti C, Bora N, Gelsomino R, Goerges S, Irlinger F, Goodfellow M, Ward AC, Vancanneyt M, Swings J, Scherer S, Guéguen M, Desmasures N. 2011. Surface microbial consortia from Livarot, a French smear-ripened cheese. Canadian Journal of Microbiology 57:651–660.

4. Lavoie K, Touchette M, St-Gelais D, Labrie S. 2012. Characterization of the fungal microflora in raw milk and specialty cheeses of the province of Quebec. Dairy Sci & Technol 92:455–468.

5. Feurer C, Irlinger F, Spinnler H e., Glaser P, Vallaeys T. 2004. Assessment of the rind microbial diversity in a farmhouse-produced vs a pasteurized industrially produced soft red-smear cheese using both cultivation and rDNA-based methods. Journal of Applied Microbiology 97:546–556.

6. Mounier J, Monnet C, Jacques N, Antoinette A, Irlinger F. 2009. Assessment of the microbial diversity at the surface of Livarot cheese using culture-dependent and independent approaches. International Journal of Food Microbiology 133:31–37.

7. Mounier J, Gelsomino R, Goerges S, Vancanneyt M, Vandemeulebroecke K, Hoste B, Scherer S, Swings J, Fitzgerald GF, Cogan TM. 2005. Surface Microflora of Four Smear-Ripened Cheeses. Appl Environ Microbiol 71:6489–6500.

598 8. Rea MC, Görges S, Gelsomino R, Brennan NM, Mounier J, Vancanneyt M, Scherer S, Swings J,
599 Cogan TM. 2007. Stability of the Biodiversity of the Surface Consortia of Gubbeen, a Red-Smear
600 Cheese. Journal of Dairy Science 90:2200–2210.

601 9. Delcenserie V, Taminiau B, Delhalle L, Nezer C, Doyen P, Crevecoeur S, Roussey D, Korsak N,
602 Daube G. 2014. Microbiota characterization of a Belgian protected designation of origin cheese,
603 Herve cheese, using metagenomic analysis. Journal of Dairy Science 97:6046–6056.

604 10. Dugat-Bony E, Garnier L, Denonfoux J, Ferreira S, Sarthou A-S, Bonnarme P, Irlinger F. 2016.
605 Highlighting the microbial diversity of 12 French cheese varieties. International Journal of Food
606 Microbiology 238:265–273.

607 11. Quigley L, O'Sullivan O, Beresford TP, Ross RP, Fitzgerald GF, Cotter PD. 2012. High-throughput
608 sequencing for detection of subpopulations of bacteria not previously associated with artisanal
609 cheeses. Applied and Environmental Microbiology 78:5717–5723.

610 12. Wolfe BE, Button JE, Santarelli M, Dutton RJ. 2014. Cheese rind communities provide tractable
611 systems for in situ and in vitro studies of microbial diversity. Cell 158:422–433.

612 13. Irlinger F, Monnet C. 2021. Temporal differences in microbial composition of Époisses cheese
613 rinds during ripening and storage. Journal of Dairy Science 104:7500–7508.

614 14. Saak CC, Pierce EC, Dinh CB, Portik D, Hall R, Ashby M, Dutton RJ. 2023. Longitudinal, Multi-
615 Platform Metagenomics Yields a High-Quality Genomic Catalog and Guides an In Vitro Model
616 for Cheese Communities. mSystems 8:e00701-22.

617 15. Kothe CI, Bolotin A, Kraïem B-F, Dridi B, Renault P. 2021. Unraveling the world of halophilic and
618 halotolerant bacteria in cheese by combining cultural, genomic and metagenomic approaches.
619 International Journal of Food Microbiology 358:109312.

620 16. Mayo B, Rodríguez J, Vázquez L, Flórez AB. 2021. Microbial Interactions within the Cheese
621 Ecosystem and Their Application to Improve Quality and Safety. 3. Foods 10:602.

622 17. De Filippis F, Genovese A, Ferranti P, Gilbert JA, Ercolini D. 2016. Metatranscriptomics reveals
623 temperature-driven functional changes in microbiome impacting cheese maturation rate. Sci
624 Rep 6.

625 18. Dugat-Bony E, Bonnarme P, Fraud S, Catellote J, Sarthou A-S, Loux V, Rué O, Bel N, Chuzeville S,
626 Helinck S. 2019. Effect of sodium chloride reduction or partial substitution with potassium
627 chloride on the microbiological, biochemical and sensory characteristics of semi-hard and soft
628 cheeses. Food Research International 125:108643.

629 19. Irlinger F, Mounier J. 2009. Microbial interactions in cheese: implications for cheese quality and
630 safety. Current Opinion in Biotechnology 20:142–148.

631 20. Kastman EK, Kamelamela N, Norville JW, Cosetta CM, Dutton RJ, Wolfe BE. 2016. Biotic
632 interactions shape the ecological distributions of Staphylococcus species. mBio 7:e01157-16.

633 21. Pham N-P, Landaud S, Lieben P, Bonnarme P, Monnet C. 2019. Transcription Profiling Reveals
634 Cooperative Metabolic Interactions in a Microbial Cheese-Ripening Community Composed of
635 Debaryomyces hansenii, Brevibacterium aurantiacum, and Hafnia alvei. Front Microbiol 10.

636 22. Brown TL, Charity OJ, Adriaenssens EM. 2022. Ecological and functional roles of bacteriophages
637 in contrasting environments: marine, terrestrial and human gut. Current Opinion in
638 Microbiology 70:102229.

639 23. Ledormand P, Desmasures N, Dalmasso M. 2020. Phage community involvement in fermented
640 beverages: an open door to technological advances? Critical Reviews in Food Science and
641 Nutrition 1–10.

642 24. Paillet T, Dugat-Bony E. 2021. Bacteriophage ecology of fermented foods: anything new under
643 the sun? Current Opinion in Food Science 40:102–111.

644 25. Garneau JE, Moineau S. 2011. Bacteriophages of lactic acid bacteria and their impact on milk
645 fermentations. Microb Cell Fact 10 Suppl 1:S20.

646 26. Pujato S a., Quiberoni A, Mercanti D j. 2019. Bacteriophages on dairy foods. Journal of Applied
647 Microbiology 126:14–30.

648 27. Marcó MB, Moineau S, Quiberoni A. 2012. Bacteriophages and dairy fermentations.
649 Bacteriophage 2:149–158.

650 28. Muhammed MK, Kot W, Neve H, Mahony J, Castro-Mejía JL, Krych L, Hansen LH, Nielsen DS,
651 Sørensen SJ, Heller KJ, Sinderen D van, Vogensen FK. 2017. Metagenomic analysis of dairy
652 bacteriophages: extraction method and pilot study on whey samples derived from using
653 undefined and defined mesophilic starter cultures. Appl Environ Microbiol 83:e00888-17.

654 29. Dugat-Bony E, Lossouarn J, De Paepe M, Sarthou A-S, Fedala Y, Petit M-A, Chaillou S. 2020. Viral
655 metagenomic analysis of the cheese surface: A comparative study of rapid procedures for
656 extracting viral particles. Food Microbiology 85:103278.

657 30. Queiroz LL, Lacorte GA, Isidorio WR, Landgraf M, de Melo Franco BDG, Pinto UM, Hoffmann C.
658 2022. High Level of Interaction between Phages and Bacteria in an Artisanal Raw Milk Cheese
659 Microbial Community. mSystems 0:e00564-22.

660 31. Cheng L, Marinelli LJ, Grosset N, Fitz-Gibbon ST, Bowman CA, Dang BQ, Russell DA, Jacobs-Sera
661 D, Shi B, Pellegrini M, Miller JF, Gautier M, Hatfull GF, Modlin RL. 2018. Complete genomic
662 sequences of Propionibacterium freudenreichii phages from Swiss cheese reveal greater
663 diversity than Cutibacterium (formerly Propionibacterium) acnes phages. BMC Microbiology
664 18:19.

665 32. de Melo AG, Rousseau GM, Tremblay DM, Labrie SJ, Moineau S. 2020. DNA tandem repeats
666 contribute to the genetic diversity of Brevibacterium aurantiacum phages. Environmental
667 Microbiology 22:3413–3428.

668 33. Gautier M, Rouault A, Sommer P, Briandet R. 1995. Occurrence of Propionibacterium
669 freudenreichii bacteriophages in swiss cheese. Appl Environ Microbiol 61:2572–2576.

670 34. Paillet T, Lossouarn J, Figueroa C, Midoux C, Rué O, Petit M-A, Dugat-Bony E. 2022. Virulent
671 Phages Isolated from a Smear-Ripened Cheese Are Also Detected in Reservoirs of the Cheese
672 Factory. 8. Viruses 14:1620.

673 35. Nayfach S, Camargo AP, Schulz F, Eloe-Fadrosh E, Roux S, Kyrpides NC. 2021. CheckV assesses
674 the quality and completeness of metagenome-assembled viral genomes. 5. Nat Biotechnol
675 39:578–585.

676 36. Kieft K, Zhou Z, Anantharaman K. 2020. VIBRANT: automated recovery, annotation and curation
677 of microbial viruses, and evaluation of viral community function from genomic sequences.
678 Microbiome 8:90.

679 37. Love MI, Huber W, Anders S. 2014. Moderated estimation of fold change and dispersion for
680 RNA-seq data with DESeq2. Genome Biology 15:550.

681 38. McMurdie PJ, Holmes S. 2014. Waste Not, Want Not: Why Rarefying Microbiome Data Is
682 Inadmissible. PLOS Computational Biology 10:e1003531.

683 39. Walsh AM, Macori G, Kilcawley KN, Cotter PD. 2020. Meta-analysis of cheese microbiomes
684 highlights contributions to multiple aspects of quality. Nat Food 1:500–510.

685 40. de Melo AG, Lemay M-L, Moineau S. 2023. The impact of Brevibacterium aurantiacum virulent
686 phages on the production of smear surface-ripened cheeses. International Journal of Food
687 Microbiology 400:110252.

688 41. De Pasquale I, Di Cagno R, Buchin S, De Angelis M, Gobbetti M. 2014. Microbial Ecology
689 Dynamics Reveal a Succession in the Core Microbiota Involved in the Ripening of Pasta Filata
690 Caciocavallo Pugliese Cheese. Applied and Environmental Microbiology 80:6243–6255.

691 42. Flórez AB, Mayo B. 2006. Microbial diversity and succession during the manufacture and
692 ripening of traditional, Spanish, blue-veined Cabrales cheese, as determined by PCR-DGGE.
693 International Journal of Food Microbiology 110:165–171.

694 43. Fuka MM, Wallisch S, Engel M, Welzl G, Havranek J, Schloter M. 2013. Dynamics of Bacterial
695 Communities during the Ripening Process of Different Croatian Cheese Types Derived from Raw
696 Ewe's Milk Cheeses. PLoS ONE 8:e80734.

697 44. Larpin S, Mondoloni C, Goerges S, Vernoux J-P, Guéguen M, Desmasures N. 2006. *Geotrichum*
698 *candidum* dominates in yeast population dynamics in Livarot, a French red-smear cheese. FEMS
699 Yeast Research 6:1243–1253.

700 45. Pangallo D, Šaková N, Koreňová J, Puškárová A, Kraková L, Valík L, Kuchta T. 2014. Microbial
701 diversity and dynamics during the production of May bryndza cheese. International Journal of
702 Food Microbiology 170:38–43.

703 46. Ortiz Charneco G, De Waal PP, Van Rijswijck IMH, Van Peij NNME, Van Sinderen D, Mahony J.
704 2023. Bacteriophages in the Dairy Industry: A Problem Solved? Annu Rev Food Sci Technol
705 14:367–385.

706 47. Somerville V, Berthoud H, Schmidt RS, Bachmann H-P, Meng YH, Fuchsmann P, von Ah U, Engel
707 P. 2021. Functional strain redundancy and persistent phage infection in Swiss hard cheese
708 starter cultures. ISME J 1–12.

709 48. Erkus O, de Jager VC, Spus M, van Alen-Boerrigter IJ, van Rijswijck IM, Hazelwood L, Janssen
710 PW, van Hijum SA, Kleerebezem M, Smid EJ. 2013. Multifactorial diversity sustains microbial
711 community stability. The ISME journal 7:2126–2136.

712 49. Spus M, Wardhana YR, Wolkers-Rooijackers JCM, Abee T, Smid EJ. 2023. Lytic bacteriophages
713 affect the population dynamics of multi-strain microbial communities. Microbiome Res Rep 2.

714 50. Jolicoeur AP, Lemay M-L, Beaubien E, Bélanger J, Bergeron C, Bourque-Leblanc F, Doré L,
715 Dupuis M-È, Fleury A, Garneau JE, Labrie SJ, Labrie S, Lacasse G, Lamontagne-Drolet M, Lessard-
716 Hurtubise R, Martel B, Menasria R, Morin-Pelchat R, Pageau G, Samson JE, Rousseau GM,
717 Tremblay DM, Duquenne M, Lamoureux M, Moineau S. 2023. Longitudinal Study of Lactococcus
718 Phages in a Canadian Cheese Factory. Applied and Environmental Microbiology 0:e00421-23.

719 51. Madera C, Monjardín C, Suárez JE. 2004. Milk contamination and resistance to processing
720 conditions determine the fate of Lactococcus lactis bacteriophages in dairies. Applied and
721 Environmental Microbiology 70:7365–7371.

722 52. Wagner N, Brinks E, Samtlebe M, Hinrichs J, Atamer Z, Kot W, Franz CMAP, Neve H, Heller KJ.
723 2017. Whey powders are a rich source and excellent storage matrix for dairy bacteriophages.
724 International Journal of Food Microbiology 241:308–317.

725 53. Bokulich NA, Mills DA. 2013. Facility-Specific “House” Microbiome Drives Microbial Landscapes
726 of Artisan Cheesemaking Plants. Applied and Environmental Microbiology 79:5214–5223.

727 54. Raymond-Fleury A, Lessard M-H, Chamberland J, Pouliot Y, Dugat-Bony E, Turgeon SL, St-Gelais
728 D, Labrie S. 2022. Analysis of Microbiota Persistence in Quebec's Terroir Cheese Using a
729 Metabarcoding Approach. 7. Microorganisms 10:1381.

730 55. Bolger AM, Lohse M, Usadel B. 2014. Trimmomatic: a flexible trimmer for Illumina sequence
731 data. Bioinformatics 30:2114–2120.

732 56. Bankevich A, Nurk S, Antipov D, Gurevich AA, Dvorkin M, Kulikov AS, Lesin VM, Nikolenko SI,
733 Pham S, Prjibelski AD, Pyshkin AV, Sirotkin AV, Vyahhi N, Tesler G, Alekseyev MA, Pevzner PA.
734 2012. SPAdes: a new genome assembly algorithm and its applications to single-cell sequencing.
735 J Comput Biol 19:455–477.

736 57. Shah SA, Deng L, Thorsen J, Pedersen AG, Dion MB, Castro-Mejía JL, Silins R, Romme FO,
737 Sausset R, Jessen LE, Ndela EO, Hjelmsø M, Rasmussen MA, Redgwell TA, Leal Rodríguez C,
738 Vestergaard G, Zhang Y, Chawes B, Bønnelykke K, Sørensen SJ, Bisgaard H, Enault F, Stokholm J,
739 Moineau S, Petit M-A, Nielsen DS. 2023. Expanding known viral diversity in the healthy infant
740 gut. 5. Nat Microbiol 8:986–998.

741 58. Kent WJ. 2002. BLAT—The BLAST-Like Alignment Tool. Genome Res 12:656–664.

742 59. Guo J, Bolduc B, Zayed AA, Varsani A, Dominguez-Huerta G, Delmont TO, Pratama AA, Gazitúa
743 MC, Vik D, Sullivan MB, Roux S. 2021. VirSorter2: a multi-classifier, expert-guided approach to
744 detect diverse DNA and RNA viruses. Microbiome 9:37.

745 60. Roux S, Camargo AP, Coutinho FH, Dabdoub SM, Dutilh BE, Nayfach S, Tritt A. 2022. iPHoP: an
746 integrated machine-learning framework to maximize host prediction for metagenome-
747 assembled virus genomes. preprint. Microbiology.

748 61. Vasimuddin Md, Misra S, Li H, Aluru S. 2019. Efficient Architecture-Aware Acceleration of BWA-
749 MEM for Multicore Systems, p. 314–324. *In* 2019 IEEE International Parallel and Distributed
750 Processing Symposium (IPDPS).

751 62. McMurdie PJ, Holmes S. 2013. phyloseq: an R package for reproducible interactive analysis and
752 graphics of microbiome census data. PLOS ONE 8:e61217.

753 63. Lin H, Peddada SD. 2020. Analysis of microbial compositions: a review of normalization and
754 differential abundance analysis. 1. npj Biofilms Microbiomes 6:1–13.

755 64. Escudié F, Auer L, Bernard M, Mariadassou M, Cauquil L, Vidal K, Maman S, Hernandez-Raquet
756 G, Combes S, Pascal G. 2017. FROGS: Find, Rapidly, OTUs with Galaxy Solution. Bioinformatics
757 https://doi.org/10.1093/bioinformatics/btx791.

758 65. Mahé F, Rognes T, Quince C, de Vargas C, Dunthorn M. 2014. Swarm: robust and fast clustering
759 method for amplicon-based studies. PeerJ 2:e593.

760 66. Bokulich NA, Subramanian S, Faith JJ, Gevers D, Gordon JI, Knight R, Mills DA, Caporaso JG.
761 2013. Quality-filtering vastly improves diversity estimates from Illumina amplicon sequencing.
762 Nat Methods 10:57–59.

763 67. Yoon S-H, Ha S-M, Kwon S, Lim J, Kim Y, Seo H, Chun J. 2017. Introducing EzBioCloud: a
764 taxonomically united database of 16S rRNA gene sequences and whole-genome assemblies. Int
765 J Syst Evol Microbiol 67:1613–1617.

766

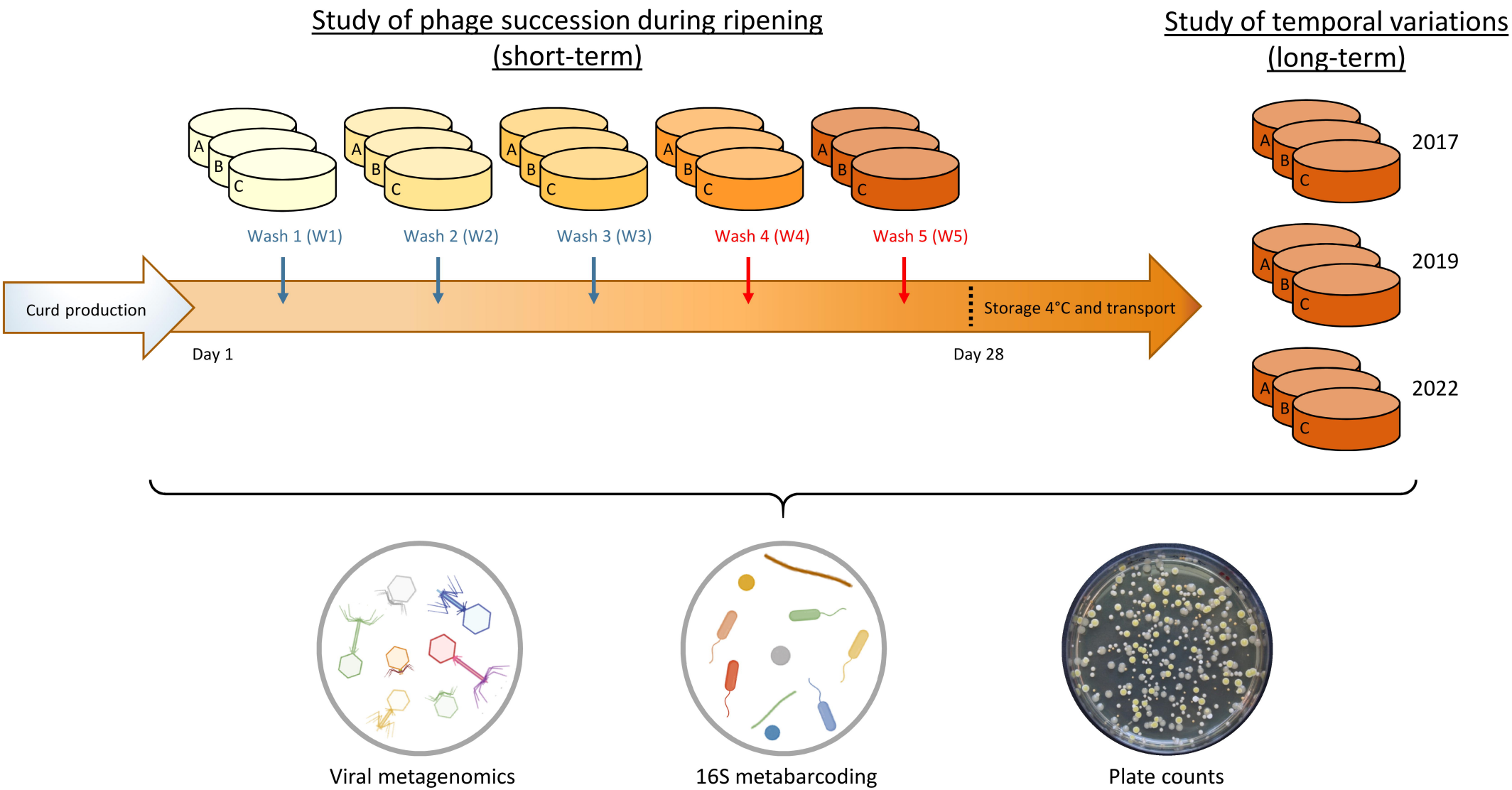
Study of phage succession during ripening (short-term)
Study of temporal variations (long-term)
A
B
C
Wash 1 (W1)
Wash 2 (W2)
Wash 3 (W3)
Wash 4 (W4)
Wash 5 (W5)
Curd production
Day 1
Day 28
Storage 4°C and transport
2017
2019
2022
Viral metagenomics
16S metabarcoding
Plate counts

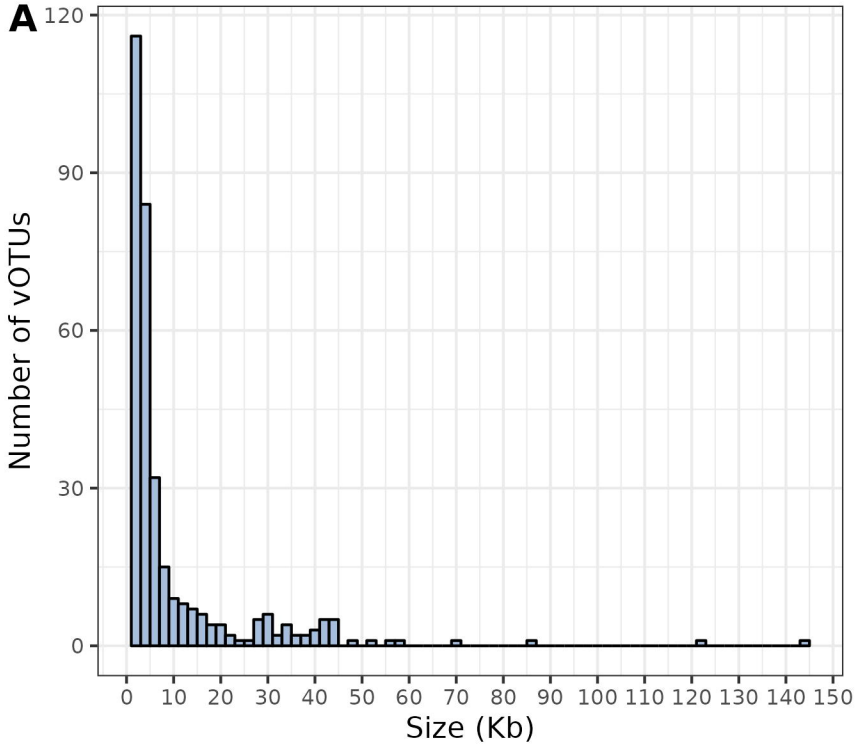
A
Number of vOTUs
120
90
60
30
0
0 10 20 30 40 50 60 70 80 90 100 110 120 130 140 150
Size (Kb)

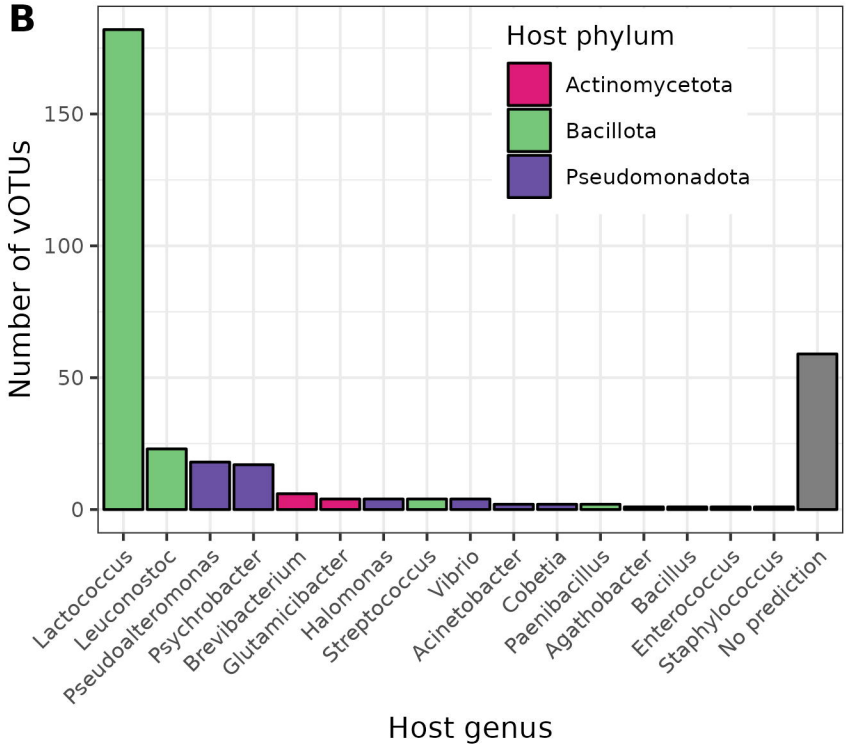
B
Host phylum
Actinomycetota
Bacillota
Pseudomonadota
Number of vOTUs
150
100
50
0
Lactococcus
Leuconostoc
Pseudoalteromonas
Psychrobacter
Brevibacterium
Glutamicibacter
Halomonas
Streptococcus
Vibrio
Acinetobacter
Cobetia
Paenibacillus
Agathobacter
Bacillus
Enterococcus
Staphylococcus
No prediction
Host genus

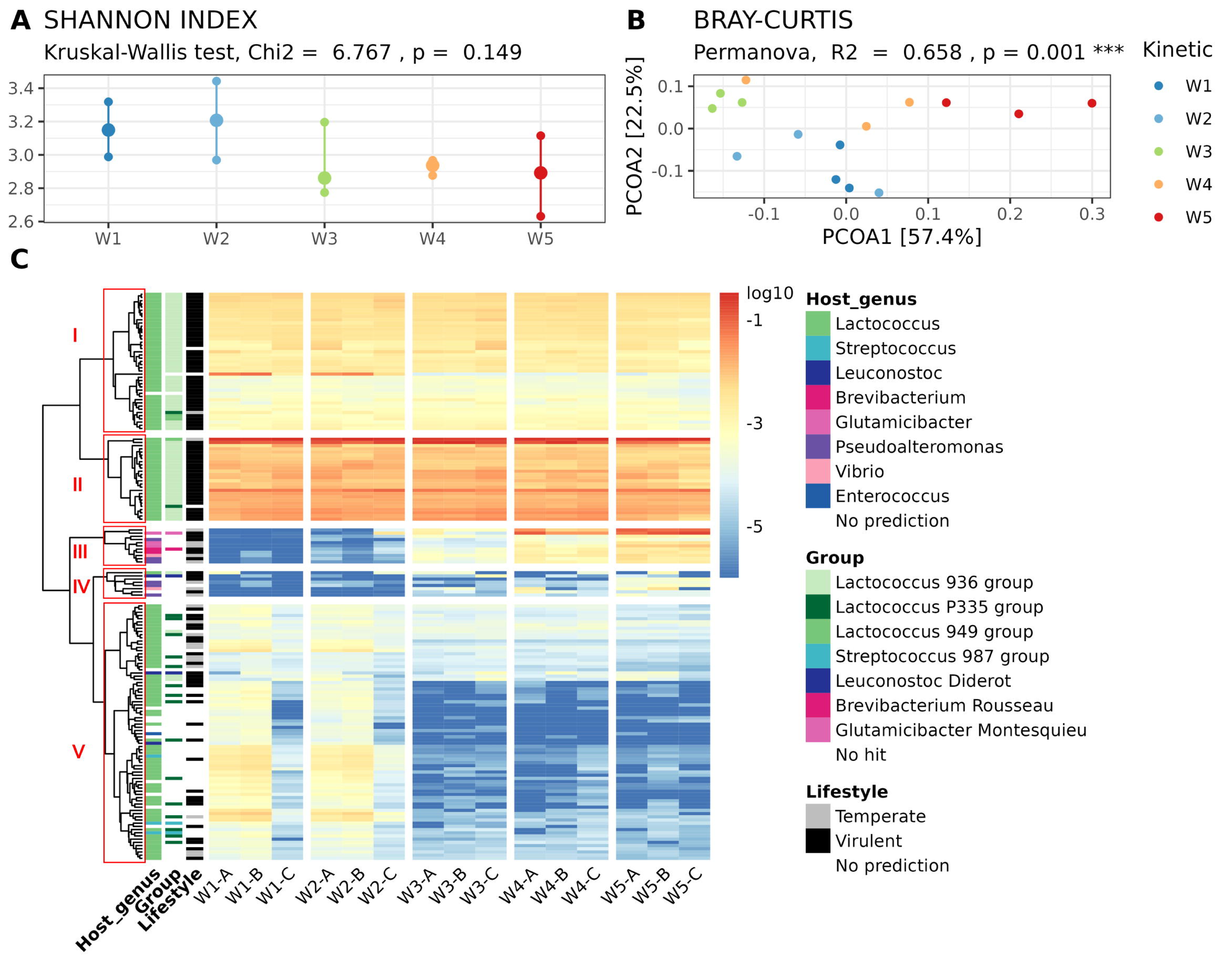
A
SHANNON INDEX
Kruskal-Wallis test, Chi2 = 6.767 , p = 0.149
3.4
3.2
3.0
2.8
2.6
W1
W2
W3
W4
W5
B
BRAY-CURTIS
Permanova, R2 = 0.658 , p = 0.001 ***
PCOA2 [22.5%]
PCOA1 [57.4%]
0.1
0.0
-0.1
-0.1
0.0
0.1
0.2
0.3
Kinetic
W1
W2
W3
W4
W5
C
I
II
III
IV
V
log10
-1
-3
-5
Host_genus
Lactococcus
Streptococcus
Leuconostoc
Brevibacterium
Glutamicibacter
Pseudoalteromonas
Vibrio
Enterococcus
No prediction
Group
Lactococcus 936 group
Lactococcus P335 group
Lactococcus 949 group
Streptococcus 987 group
Leuconostoc Diderot
Brevibacterium Rousseau
Glutamicibacter Montesquieu
No hit
Lifestyle
Temperate
Virulent
No prediction
Host_genus
Group
Lifestyle
W1-A
W1-B
W1-C
W2-A
W2-B
W2-C
W3-A
W3-B
W3-C
W4-A
W4-B
W4-C
W5-A
W5-B
W5-C

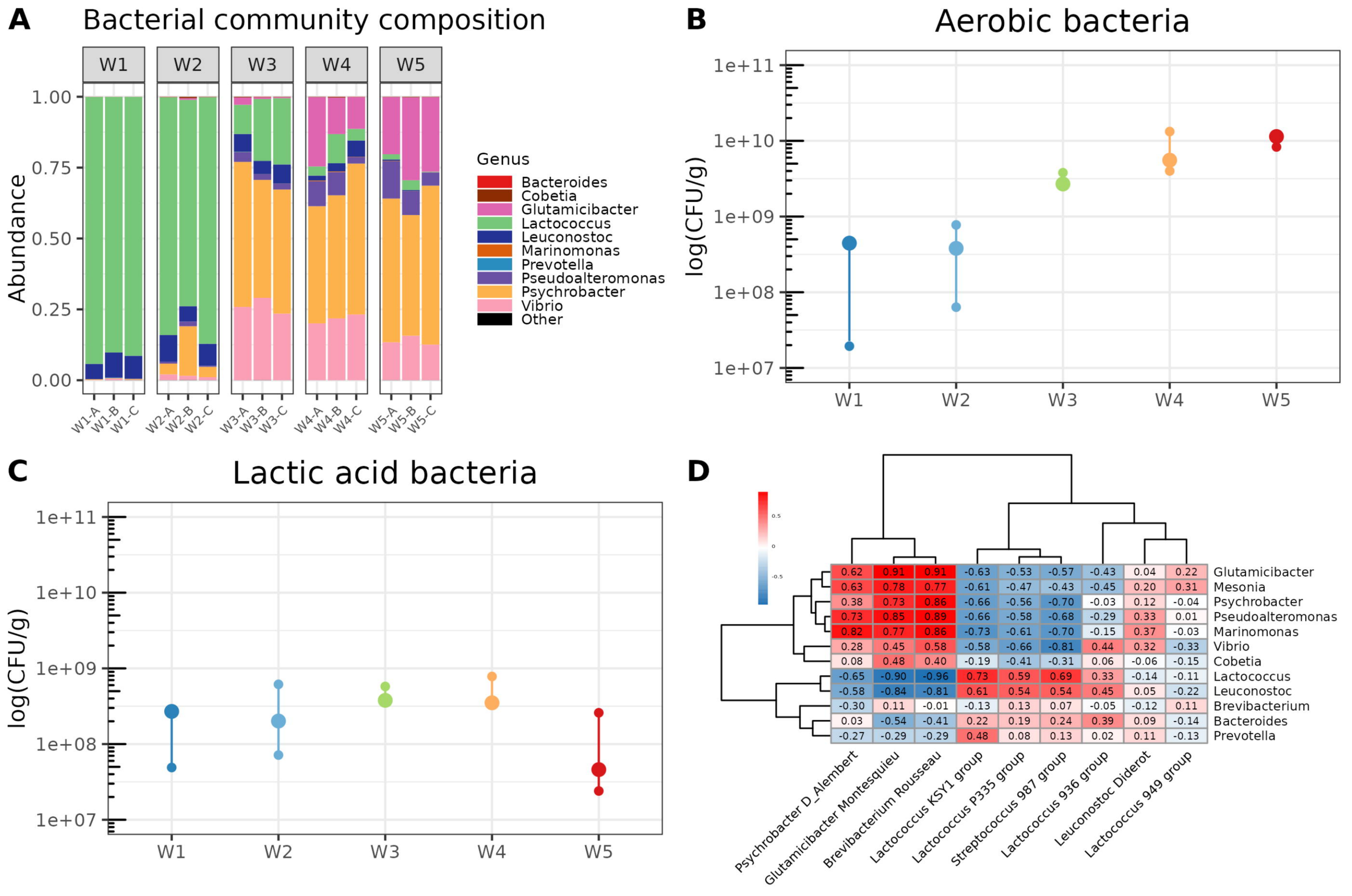
A
Bacterial community composition
W1
W2
W3
W4
W5
Abundance
1.00
0.75
0.50
0.25
0.00
W1-A
W1-B
W1-C
W2-A
W2-B
W2-C
W3-A
W3-B
W3-C
W4-A
W4-B
W4-C
W5-A
W5-B
W5-C
Genus
Bacteroides
Cobetia
Glutamicibacter
Lactococcus
Leuconostoc
Marinomonas
Prevotella
Pseudoalteromonas
Psychrobacter
Vibrio
Other
B
Aerobic bacteria
log(CFU/g)
1e+11
1e+10
1e+09
1e+08
1e+07
W1
W2
W3
W4
W5
C
Lactic acid bacteria
log(CFU/g)
1e+11
1e+10
1e+09
1e+08
1e+07
W1
W2
W3
W4
W5
D
0.5
0
-0.5
Glutamicibacter 0.62 0.91 0.91 -0.63 -0.53 -0.57 -0.43 0.04 0.22
Mesonia 0.63 0.78 0.77 -0.61 -0.47 -0.43 -0.45 0.20 0.31
Psychrobacter 0.38 0.73 0.86 -0.66 -0.56 -0.70 -0.03 0.12 -0.04
Pseudoalteromonas 0.73 0.85 0.89 -0.66 -0.58 -0.68 -0.29 0.33 0.01
Marinomonas 0.82 0.77 0.86 -0.73 -0.61 -0.70 -0.15 0.37 -0.03
Vibrio 0.28 0.45 0.58 -0.58 -0.66 -0.81 0.44 0.32 -0.33
Cobetia 0.08 0.48 0.40 -0.19 -0.41 -0.31 0.06 -0.06 -0.15
Lactococcus -0.65 -0.90 -0.96 0.73 0.59 0.69 0.33 -0.14 -0.11
Leuconostoc -0.58 -0.84 -0.81 0.61 0.54 0.54 0.45 0.05 -0.22
Brevibacterium -0.30 0.11 -0.01 -0.13 0.13 0.07 -0.05 -0.12 0.11
Bacteroides 0.03 -0.54 -0.41 0.22 0.19 0.24 0.39 0.09 -0.14
Prevotella -0.27 -0.29 -0.29 0.48 0.08 0.13 0.02 0.11 -0.13
Psychrobacter D_Alembert
Glutamicibacter Montesquieu
Brevibacterium Rousseau
Lactococcus KSY1 group
Lactococcus P335 group
Streptococcus 987 group
Lactococcus 936 group
Leuconostoc Diderot
Lactococcus 949 group

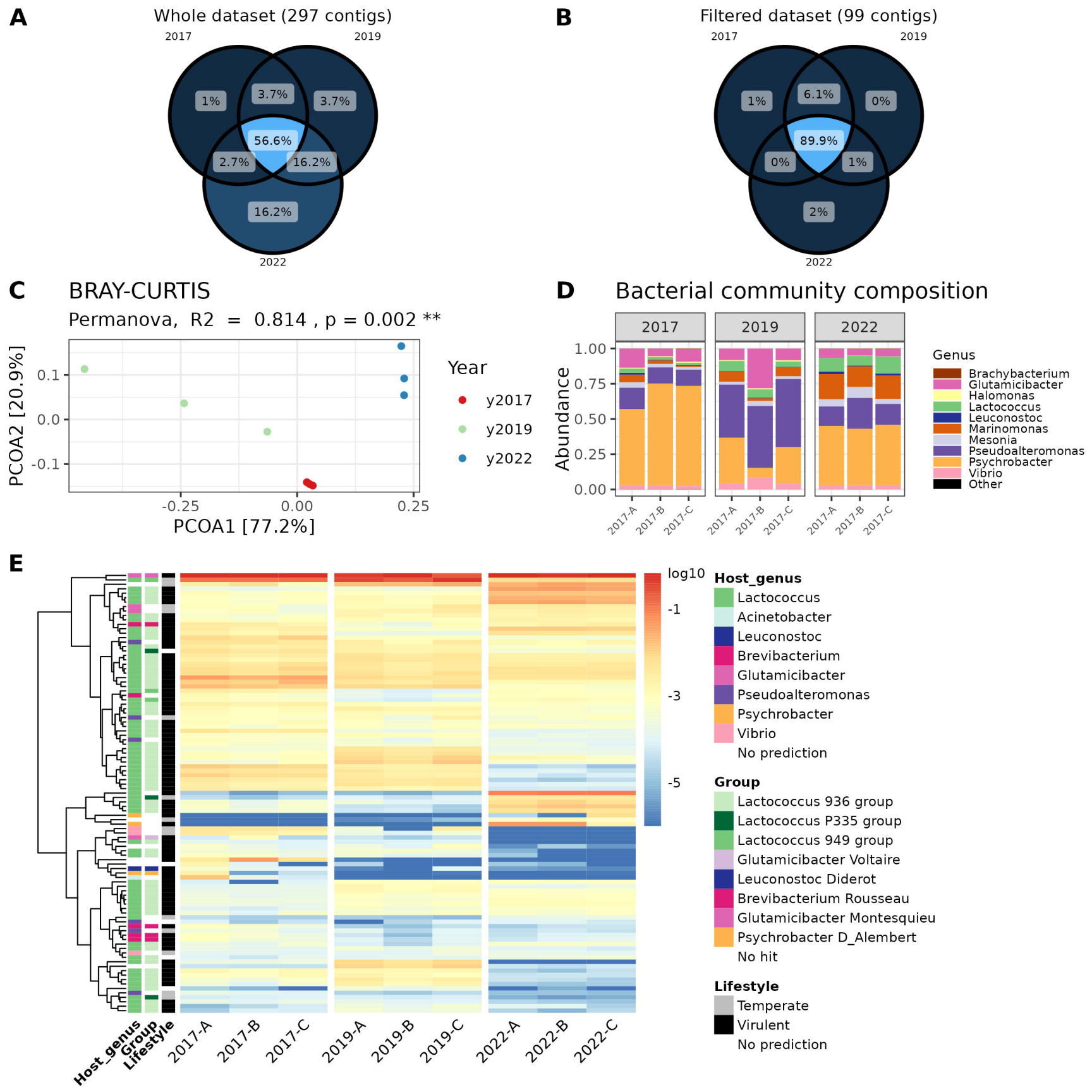
A
Whole dataset (297 contigs)
2017
2019
2022
1%
3.7%
3.7%
56.6%
2.7%
16.2%
16.2%
B
Filtered dataset (99 contigs)
2017
2019
2022
1%
6.1%
0%
89.9%
0%
1%
2%
C
BRAY-CURTIS
Permanova, R2 = 0.814 , p = 0.002 **
PCOA2 [20.9%]
PCOA1 [77.2%]
0.1
0.0
-0.1
-0.25
0.00
0.25
Year
y2017
y2019
y2022
D
Bacterial community composition
2017
2019
2022
Abundance
1.00
0.75
0.50
0.25
0.00
2017-A
2017-B
2017-C
Genus
Brachybacterium
Glutamicibacter
Halomonas
Lactococcus
Leuconostoc
Marinomonas
Mesonia
Pseudoalteromonas
Psychrobacter
Vibrio
Other
E
log10
-1
-3
-5
Host_genus
Lactococcus
Acinetobacter
Leuconostoc
Brevibacterium
Glutamicibacter
Pseudoalteromonas
Psychrobacter
Vibrio
No prediction
Group
Lactococcus 936 group
Lactococcus P335 group
Lactococcus 949 group
Glutamicibacter Voltaire
Leuconostoc Diderot
Brevibacterium Rousseau
Glutamicibacter Montesquieu
Psychrobacter D_Alembert
No hit
Lifestyle
Temperate
Virulent
No prediction
Host_genus
Group
Lifestyle
2017-A
2017-B
2017-C
2019-A
2019-B
2019-C
2022-A
2022-B
2022-C